AGU PUBLICATIONS

Geophysical Research Letters

RESEARCH LETTER

10.1002/2016GL070893

Key Points:
- Both rain evaporation and surface fluxes are important for generating moist patches
- Importance of rain evaporation decreases with height
- Thermodynamic forcing is more sensitive to environmental variables than previously thought

Supporting Information:
- Supporting Information S1

Correspondence to:
G. Torri,
torri@fas.harvard.edu

Citation:
Torri, G., and Z. Kuang (2016), Rain evaporation and moist patches in tropical boundary layers, *Geophys. Res. Lett.*, *43*, doi:10.1002/2016GL070893.

Received 28 JUL 2016
Accepted 26 AUG 2016
Accepted article online 31 AUG 2016

Rain evaporation and moist patches in tropical boundary layers

Giuseppe Torri[1] and Zhiming Kuang[1,2]

[1]Department of Earth and Planetary Sciences, Harvard University, Cambridge, Massachusetts, USA, [2]Harvard John A. Paulson School of Engineering and Applied Sciences, Harvard University, Cambridge, Massachusetts, USA

Abstract Moist patches are areas in the subcloud layer characterized by a positive water vapor anomaly compared to the environment and are considered important in triggering new convective cells. A correct understanding of the origin of the water vapor in these patches is, thus, essential to improving existing convective parameterizations. Recent studies have addressed this problem and have shown that contrary to what was previously thought, the main source of water vapor in moist patches are surface latent heat fluxes, instead of rain evaporation. This manuscript offers a different perspective to the topic, focusing on the origin only of the water vapor that makes moist patches anomalously moist when compared to the environment. It is found that near the surface, rain evaporation contributes half as much as latent heat fluxes, implying that a parameterization of the thermodynamic forcing should be more sensitive to environmental variables, like relative humidity, than recently suggested.

1. Introduction

The role of cold pools in triggering new convective clouds has been known for a long time. The principal mechanism that was initially recognized as responsible for the triggering was the forced lifting of environmental air by the gust fronts of propagating cold pools [*Purdom*, 1976; *Weaver and Nelson*, 1982], which could happen either as a result of cold pool collisions or through the interaction between the cold pools' gust fronts and the environmental wind. This type of forcing, which we will refer to as *mechanical*, was typically observed in the presence of large-scale organization [see, e.g., *Knupp and Cotton*, 1982; *Droegemeier and Wilhelmson*, 1985a, 1985b; *Rotunno and Klemp*, 1985; *Rotunno et al.*, 1988; *Weisman et al.*, 1988; *Weisman and Rotunno*, 2004], where cold pools tend to have strong gust fronts and the wind shear can be considerable.

For cases with no large-scale organization, which are often found over the tropical ocean, another mechanism was proposed more recently. Examining a series of simulations over a warm ocean and with low vertical wind shear, *Tompkins* [2001] hypothesized that parcels reaching their level of free convection originate at the surface from areas around cold pools that exhibit a positive equivalent potential temperature, θ_e, anomaly, which we shall call *moist patches*. Their enhanced moisture content would act both to increase the parcels' buoyancy in the subcloud layer and to reduce the convective inhibition (CIN) they would experience in the inhibition layer and would thus provide them with a strong advantage compared to those in the environment. This kind of forcing, here referred to as *thermodynamic*, differs from the one discussed in the previous paragraph also because gust fronts are supposed to play very little role.

Recently, it was shown that contrary to Tompkins' hypothesis, mechanical forcing does play an important role in triggering new convective cells even in the absence of large-scale organization [*Torri et al.*, 2015; *Jeevanjee and Romps*, 2015]: because the effective buoyancy experienced by parcels throughout their ascent in the subcloud layer is small, the cold pool gust fronts are essential for lifting parcels from the surface. In spite of this partial revisitation of Tompkins' proposal, the thermodynamic advantage provided by the moist patches was nevertheless confirmed to be very important in reducing the CIN encountered by ascending parcels [*Torri et al.*, 2015].

There follows that the study of the thermodynamic forcing and, particularly, of moist patches is an essential step to take in order to gain a better understanding of deep convection in tropical environments. In this context, an important problem that has recently attracted attention is the attribution of the origin of water vapor in the moist patches.

For some time, the leading hypothesis was proposed by *Tompkins* [2001], who, through a combination of numerical simulations and observations of a severe thunderstorm by *Betts* [1984], suggested that the positive moisture anomaly surrounding cold pools is largely due to rain evaporation in the subcloud layer. This idea found support in *Seifert and Heus* [2013], who considered numerical simulations of cold pools generated by trade wind cumulus clouds. Interestingly, *Li et al.* [2014] considered a similar scenario but found no evidence of rain evaporation playing an important role in the formation of moist patches. More recently, the question was examined in two studies [*Schlemmer and Hohenegger*, 2015; *Langhans and Romps*, 2015] that reached opposite conclusions from *Tompkins* [2001]: the majority of the moisture in moist patches is to be attributed to latent heat fluxes from the ocean.

We would like to approach this problem with a different angle than the ones discussed above. Because moist patches are defined as anomalies with respect to a reference state, the important question to address is not so much about the origin of all the water vapor that particles in moist patches accumulated throughout their history in cold pools or in precipitation-driven downdrafts but, rather, that of the excess that makes the particles anomalously moist compared to the environment. In other words, we are not concerned with why moist patches are moist but, rather, why they are moist*er*.

2. Methods

The numerical model used for the simulations discussed in this manuscript is the System for Atmospheric Modeling (SAM), which solves the anelastic equations of motion and uses liquid water static energy and nonprecipitating and precipitating total water as thermodynamic prognostic variables [*Khairoutdinov and Randall*, 2003]. The equations are solved using doubly periodic boundary conditions in the horizontal directions. A prognostic turbulent kinetic energy 1.5-order closure scheme is used to parameterize subgrid scale effects.

The model is run with the Lin microphysics scheme, a single-moment scheme that predicts the specific humidities of water vapor, cloud liquid water, cloud ice, rain, snow, and graupel [*Lin et al.*, 1983]. Results from sensitivity tests obtained from a two-moment microphysics scheme [*Morrison et al.*, 2005] are discussed in Text S1 in the supporting information. There, we show that varying the concentration of cloud condensation nuclei leads to different rain evaporation rates in the lowest troposphere, which, in turn, has a strong impact on the contribution of rain evaporation to the moist patches: decreasing evaporation results in such contribution becoming almost negligible at all heights. Therefore, we suggest that the microphysics scheme used affects our results primarily through its effect on the amount of rain evaporation experienced by air parcels descending in precipitation-driven downdrafts. Different environmental soundings can similarly affect our results by changing rain evaporation, the details of which will be investigated in future studies.

The simulated domain measures 96×96 km^2 in the horizontal and 30 km in the vertical directions. The grid size in the horizontal directions is set to 250 m, whereas it varies in the vertical: 500 m above 10 km, with a progressive decrease to 31 m close to the model surface. The time step is 3 s. The simulations are carried out over an ocean with sea surface temperature held constant at 302.65 K. The diurnal cycle is removed by fixing the zenith angle at 51.7° with the solar constant halved to 685 W m^{-2}. The mean winds are initialized to zero. The surface fluxes are computed using the Monin-Obukhov similarity theory.

The numerical model is run along with the Lagrangian Particle Dispersion Model (LPDM) introduced in *Nie and Kuang* [2012]. We refer the reader to Text S2 in the supporting information for further details about the model. For every column in the domain, the LPDM is initialized with 950 particles, their positions being distributed randomly over the bottom 15 km of the model domain, with a probability distribution that is a uniform function of pressure. At every time step, we determine the water vapor acquired by each particle through rain evaporation and through surface latent heat fluxes by considering the evaporative tendencies and the diffusive tendencies near the surface provided by SAM in the grid box the particle belongs to. Every minute of model time, we record the three-dimensional fields from SAM, the positions of the Lagrangian particles, and the water vapor accumulated within that minute from the different sources mentioned above.

We first ran the model for 30 days without Lagrangian particles on the same domain until radiative-convective equilibrium (RCE) was reached. At the end of this period, we restarted the simulation with the Lagrangian particles and collected data for 12 h of model time. No nudging was imposed on the horizontal winds. The precipitation rate averaged in time during the 12 h of data collection and in space over the entire domain is 3.3 mm d^{-1}.

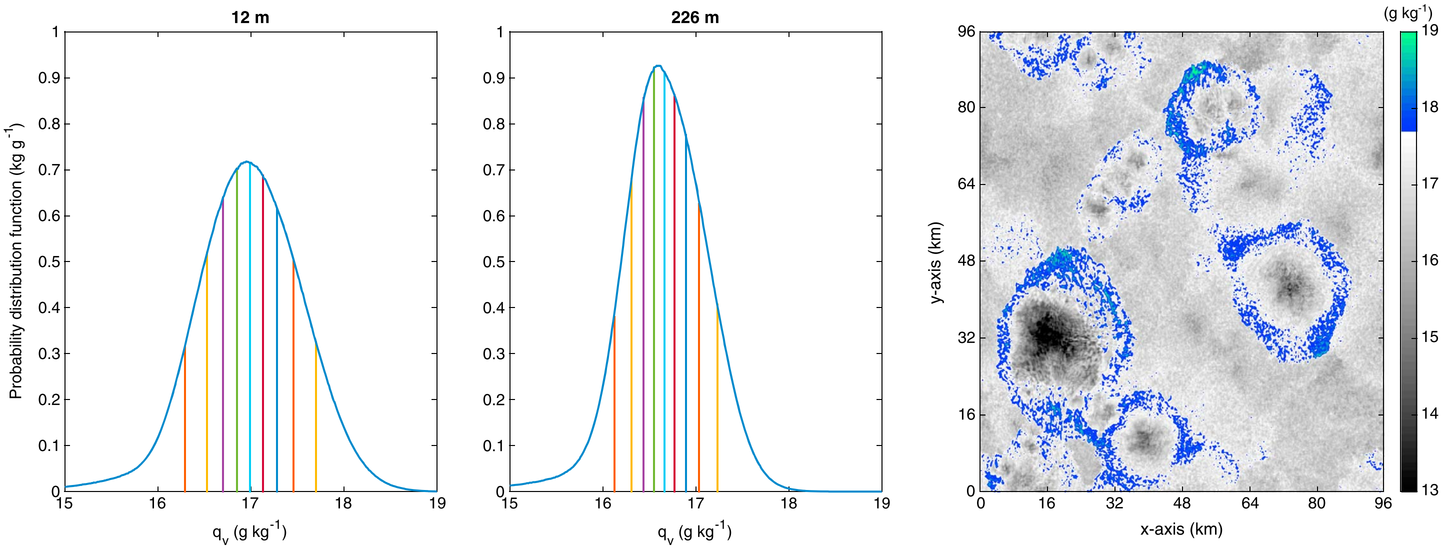

Figure 1. (left and middle) Probability distribution function of q_v at two heights, 12 m and 226 m, with the vertical lines separating the 10 different particle groups. (right) Snapshot of horizontal section of q_v at 12 m. The two different color bars merge at a value corresponding to the 90th percentile of q_v at this height.

Throughout this manuscript, we will often refer to the concept of *subcloud layer*. We define this as the portion of the model domain which includes the surface and in which the time- and domain-averaged cloud liquid water specific humidity, q_l, is below 10^{-5} g kg^{-1}. With the settings described above, this corresponds to the bottom 531 m of the domain.

Cold pools in our model are identified and tracked with the algorithm described in *Torri et al.* [2015]. In order to provide the reader with a reference, by comparing a number of vertical profiles of θ_ρ in cold pools with profiles in the environment, we estimate the typical height of the cold pool to be between 300 m and 350 m.

Another concept that we will often refer to and which is key for this study is that of *moist patch*. Instead of adopting a dichotomous definition based on some arbitrary threshold—as, e.g., in *Schlemmer and Hohenegger* [2015]—we choose to identify moist patches simply as the highest percentiles of the distribution of water vapor. In order to construct this distribution, we first scan through every time step of the model output and collect all values of q_v for each height. Then, we divide this distribution into 10 intervals—which we will call *particle groups*—per height, with the criterion that each group contains the same number of sampled values at the same altitude. One of the advantages of this procedure is that it prevents us from overweighing the tails of the distribution and ensures that each group contains a statistically significant number of grid boxes to examine. Lagrangian particles are classified according to what group the grid box they are contained belongs to. As an illustration, the 10 particle groups for two heights, 12 m and 226 m, are shown in Figure 1 (left and middle). We choose to focus on these two levels because their separation provides a good sense of how our conclusions might vary with increasing height. To give a sense of the spatial structure of the moist patches, Figure 1 (right) shows the horizontal section of q_v at 12 m from the model surface using two different color bars. The separating value between the different color bars is at 17.7 g kg^{-1}, and it corresponds to the 90th percentile of the distribution of q_v at this altitude. By definition, there follows that particles contained in any of the colored grid boxes belong to particle group 10.

We also define three particles' categories that we will use to check the consistency of the main thesis of this work: UDN, containing particles that are either in a precipitation-driven downdraft or in a cold pool after having been in a precipitation-driven downdraft; ENT, which encloses particles that have been entrained into a cold pool from the environment; OUT, which represents particles in the environment. Initially, all particles are put in the OUT category. If a particle is in a grid box with negative vertical velocity and for which the specific humidity of the precipitating condensate, q_p, is greater than 10^{-4} g kg^{-1}, then the particle is put in the UDN category. If a particle from the OUT category enters a cold pool, then it is put in the ENT category.

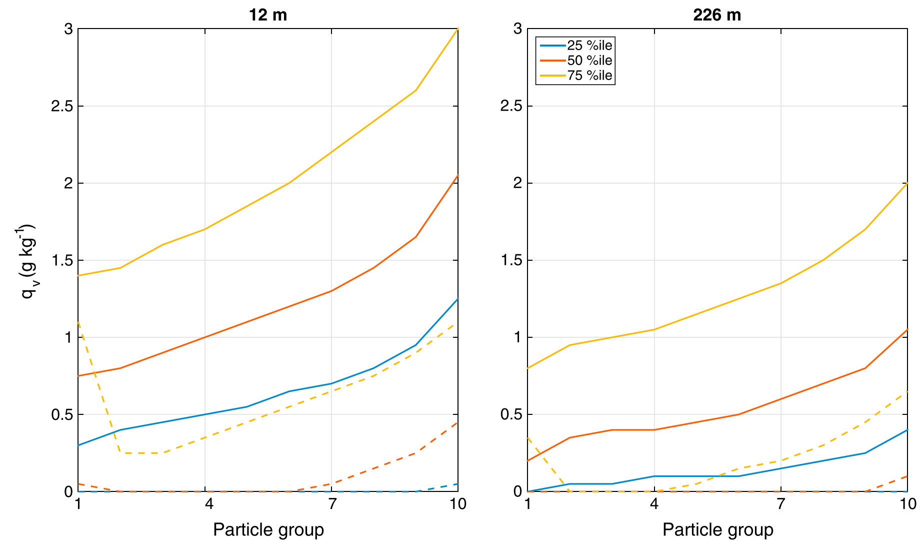

Figure 2. Different percentiles of distributions of q_{ev} (dashed lines) and q_{fl} (continuous lines) for varying particle groups. The results at (left) 12 m and (right) 226 m.

If a UDN or an ENT particle is out of a cold pool for more than 20 min, then the particle is put in the OUT category again. The same is done for UDN particles that have not entered a cold pool yet and which are out of a precipitation-driven downdraft for more than 20 min. This threshold was chosen by examining UDN and ENT particles after they left cold pools (or precipitation-driven downdrafts) and considering how much time it took their distributions of temperature and water vapor to overlap with the same distributions constructed using OUT particles. We have tested our results against different choices of threshold (15, 25, and 30 min) and found no significant differences.

3. Results

Because we are considering a case with no large-scale forcing, the only sources of q_v for particles in the subcloud layer are surface latent heat fluxes and rain evaporation. Sublimation or evaporation of melted snow and graupel could in principle play a role, but it was shown in *Torri and Kuang* [2015] that particles reaching the subcloud layer in precipitation-driven downdrafts receive very little water vapor from these microphysical processes.

In order to assess the role of the two acknowledged sources in providing the excess q_v to moist patches, we want to compare the distributions of collected water vapor for particles belonging to different particle groups. More precisely, for every particle in the last 6 h of the simulation, we consider its previous history for 6 h and record the water vapor accumulated through rain evaporation, q_{ev}, and that accumulated either through latent heat fluxes experienced at the bottom layer or through turbulent diffusion in the layers above, q_{fl}. Notice that we examine only a finite temporal window to ensure that all particles' histories are considered on an equal footing. Because we expect a considerable amount of particles in moist patches to come from a cold pool and, before then, a precipitation-driven downdraft, we use a temporal window of 6 h to guarantee that all these steps are taken into account. We also verified that our results are robust by considering a shorter window of 4 h and a longer one of 10 h.

In each panel of Figure 2 we represent the distribution of q_{ev} (dashed lines) and q_{fl} (continuous lines) for different particle groups; Figure 2 (left) shows results relative to a level near the surface, at 12 m, whereas Figure 2 (right) shows those at 226 m. In the interest of simplicity and to keep the figure as clean as possible, we have reported only the 25th, 50th, and 75th percentiles of the distributions.

As one would expect, the contributions from either sources get bigger as higher particle groups are considered. This increase is monotonic everywhere expect for q_{ev} in group 1. This group contains mostly particles entering the subcloud layer in precipitation-driven downdrafts, generally dry features, so considerable amounts of q_{ev} should be expected. An important thing to notice is that in accordance to what has been reported by other authors [*Schlemmer and Hohenegger*, 2015; *Langhans and Romps*, 2015], surface fluxes

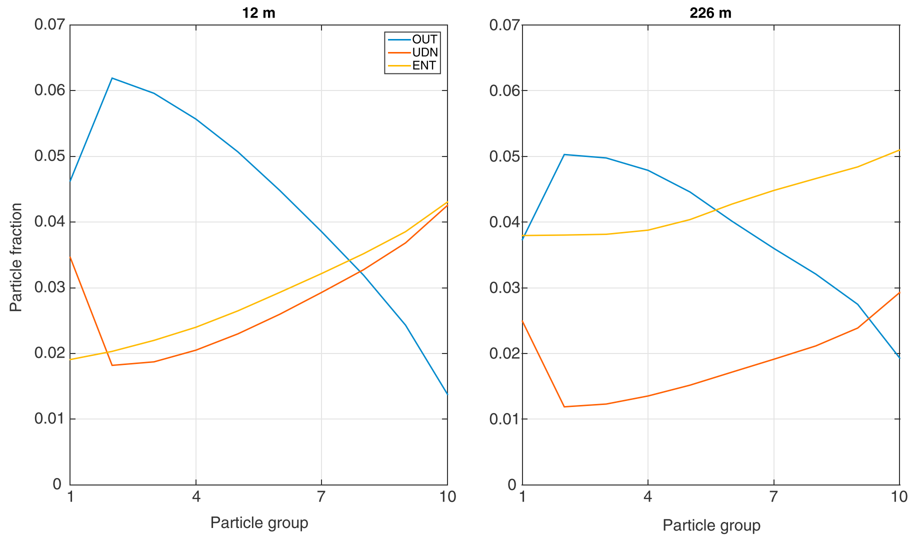

Figure 3. Normalized distributions of particles belonging to different categories—OUT, UDN, and ENT—for all particle groups at two different heights: the distributions at (left) 12 m and (right) 226 m.

represent the biggest source of moisture at different heights and for any particle group. However, if we now consider the question of what provides the excess water vapor that characterizes moist patches, the conclusions are slightly different. In particular, if we focus on the distributions at 12 m and look at the differences between particle group 10 and, e.g., particle group 6—which we can think of as representative of conditions within the environment—we notice that rain evaporation and surface fluxes contribute in similar manners: for instance, the difference in the 50th percentile between particle groups 10 and 6 amounts to 0.45 g kg^{-1} for the distribution of q_{ev} and 0.85 g kg^{-1} for the distribution of q_{fl}. At 226 m, the role of rain evaporation is overall attenuated, except for the higher percentiles of the distributions. The picture that emerges from these results is, therefore, one where rain evaporation contributes in similar amounts to latent heat fluxes in providing the extra water vapor that makes the moist patches anomalously moist. Only with increasing height do latent heat fluxes become the dominant factor.

Using the LPDM, we have also quantified the contributions from the advection scheme used in the Eulerian model. The results show that although the absolute values of such contributions are fairly high, they are roughly constant across different particle groups and, therefore, do not contribute to the water vapor anomaly that characterizes the moist patches. For more details, we refer the reader to the supporting information.

In order to better understand the picture described above and also check its consistency, we consider the history of the Lagrangian particles a bit further. In particular, we invoke the classification described in section 2 to determine the category to which each particle belongs. The panels in Figure 3 show the normalized distributions of particles' categories at two different heights—the same as those considered in Figure 2—for various particle groups.

Notice that comparing the distributions at 12 m and at 226 m, the fraction of ENT and UDN particles is very different, especially for groups corresponding to high moisture content. In particular, the figure seems to suggest that near the surface, the ratio of particles coming from precipitation-driven downdrafts over particles being entrained into a cold pool from the environment is roughly equal to one; few hundred meters above, on the other hand, the ratio has dropped to almost one half.

Let us now concentrate on the highest particle group, the tenth, and divide the amount of water vapor collected by particles across the different categories. Near the surface, at 12 m, the median q_{ev} for UDN particles is 0.90 g kg^{-1}, and the median q_{fl} equals 2.21 g kg^{-1}. For ENT particles, the median q_{ev} and q_{fl} are 0.28 g kg^{-1}, 1.90 g kg^{-1}, respectively. Finally, for OUT particles, the median q_{ev} equals 0.04 g kg^{-1}, and the median q_{fl} equals 1.89 g kg^{-1}. At 226 m, although the magnitudes are slightly smaller, the situation is essentially the same: most q_{ev} in the particle group we are considering is contributed by UDN particles—which is fairly reasonable to expect—and q_{fl} is very similar across the three categories of particles. If we combine this with the findings presented in Figure 3, the natural conclusion to draw is that rain evaporation contributes less to the

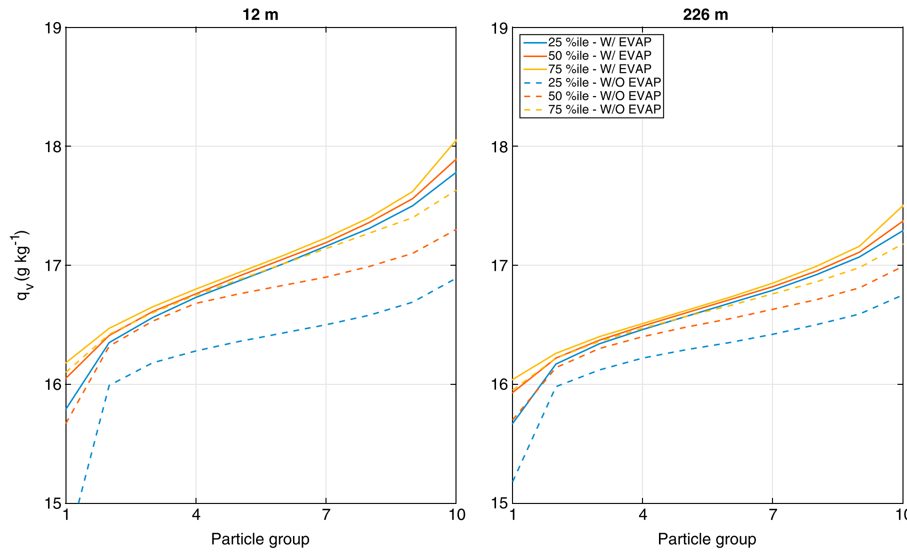

Figure 4. Comparisons at (left) 12 m and (right) 226 m between different percentiles of the distributions of the actual values of q_v (continuous lines) for grid boxes in various particle groups and the q_v they would have if the moisture accumulated through rain evaporation were to be removed (dashed lines).

moist patches in the middle of the subcloud layer because the fraction of particles that descended through a precipitation-driven downdraft—and which, therefore, experienced considerable rain evaporation— is much less than the fraction at the surface. We hypothesize that this situation is mainly due to two factors: first, that the cold pool air parcels at 226 m are closer to the interface between the cold pool and the environment and are, therefore, more exposed to dilution by entrainment than particles near the surface; furthermore, because particles coming from precipitation-driven downdrafts are embedded in air parcels which are much denser than those containing particles entrained from the environment, they are more likely to be found near the surface.

Finally, we want to discuss another consistency check for our main thesis. In order to assess the importance of rain evaporation in generating moist patches, at every time step and for each Lagrangian particle, we subtract the amount of water vapor that the particle collected in the previous 6 h through rain evaporation. Then, for every grid box, we compute the average q_v of the particles it contains, which we interpret as the Eulerian value of water vapor the grid box would have in the absence of rain evaporation. Finally, we compare the distributions of q_v with and without subtracting rain evaporation. The results for the two altitudes that we have been focusing on so far are shown in Figure 4, which is constructed much in the same spirit as Figure 2: the grid boxes at each level are sampled according to the particle group they belong to; then, for each group, we determine the distribution of the actual values of q_v and the values each grid box would have if the moisture accumulated through rain evaporation were to be subtracted. For each distribution, we show the 25th, 50th, and 75th percentiles.

At 12 m, the difference in the 50th percentile of the distribution of q_v between particle group 10 and particle group 6 amounts to 0.84 g kg^{-1}, and it is reduced to 0.47 g kg^{-1} if rain evaporation is not taken into account: as expected, the difference between the two particle groups—which could be thought of as an estimate of the magnitude of the water vapor anomaly associated with moist patches—is sensibly reduced by neglecting rain evaporation. Also as expected, note that this drop is smaller when considering a greater height: at 226 m, the difference between the aforementioned particle groups goes from 0.66 g kg^{-1} to 0.45 g kg^{-1} when rain evaporation is subtracted.

Another interesting feature of Figure 4 is that when rain evaporation is neglected, the 25th percentile of q_v seems to be shifted a lot more than the other percentiles across the various particle groups. We hypothesize this is the case because, for each particle group, the lowest percentiles of the distribution of water vapor are contributed by particles coming from greater altitudes and which, therefore, experience more rain evaporation than particles in the highest percentiles of the distribution.

Before concluding, we would like to stress that these last results should be taken with a grain of salt. In fact, in the absence of rain evaporation, precipitation-driven downdrafts would be much drier when they reach the surface than the present case and would thus give rise to bigger surface latent heat fluxes that would, to some extent, compensate for the absence of evaporated condensate.

4. Conclusions

This manuscript has focused on the moist patches in tropical boundary layers in deep convective scenarios. Contrary to few recent studies that have investigated the origin of the water vapor in these patches [*Schlemmer and Hohenegger*, 2015; *Langhans and Romps*, 2015], the present work has addressed the problem of what provides the extra water vapor that makes the patches anomalously moist areas in the subcloud layer, a particularly relevant question for formulating parameterizations of the thermodynamic forcing. Results have been obtained with an LPDM, run in RCE configuration over a warm ocean without large-scale winds.

At every time step, the water vapor accumulated by each particle through rain evaporation and surface latent heat fluxes is recorded for each Lagrangian particle. For every height in the subcloud layer, grid boxes are then sampled according to their q_v in 10 different groups in such a way that each group contains the same amounts of boxes. Particles are then classified according to what group the grid box in which they are contained belongs to. Comparison between different percentiles of the distributions of water vapor collected through different sources across all particle groups shows that although surface latent heat fluxes provide more water vapor to particles in the moist patches than rain evaporation, the two sources contribute in similar manner in providing the positive water vapor anomaly to moist patches near the surface. As height increases, the role of evaporation diminishes and the anomalous moisture content is to be ascribed mostly to surface fluxes.

As a first consistency check to this claim, the history of particles in moist patches — identified with the highest particle groups — is analyzed. Results show that near the surface, a considerable fraction of particles in moist patches comes from the precipitation-driven downdraft that has originated the cold pool and have, therefore, accumulated great amounts of water vapor through rain evaporation. At greater heights, the moist patches contain mostly particles entrained in the cold pool from the environment, which have accumulated moisture primarily through surface fluxes.

As a second consistency check, the distribution of the values of grid boxes' q_v was compared with a similar distribution where the moisture accumulated by rain evaporation was subtracted. The results show that the water vapor content of grid boxes belonging to high particle groups was sensibly reduced compared to that of boxes in lower particles groups. This difference is attenuated for increasing height.

The results presented in this work suggest that although — as also shown in the above-cited studies — surface fluxes are the main sources of water vapor for moist patches, the role of rain evaporation in generating the positive moisture anomaly associated with the moist patches is as important as that of the surface fluxes in the layers close to the surface. These findings can have important repercussions for convective parameterizations as they show that the thermodynamic forcing at the surface is more sensitive to environmental variables, like relative humidity, as previous results suggest.

Acknowledgments
The authors thank Marat Khairoutdinov for access to the SAM code, Fuqing Zhang and Martin Singh for useful discussions, and Paul Edmon for precious and tireless assistance with the Harvard Odyssey cluster on which the simulations were run. This research was partially supported by the Foundation Blanceflor Boncompagni Ludovisi née Bildt, the Office of Biological and Environmental Research of the U.S. Department of Energy under grants DE-SC0008679 as part of the ASR program, and by NSF grants AGS-1062016 and AGS-1260380. The data for this paper are available upon request.

References

Betts, A. K. (1984), Boundary layer thermodynamics of a high plains severe storm, *Mon. Weather Rev.*, *112*(11), 2199–2211, doi:10.1175/1520-0493(1984)112<2199:BLTOAH>2.0.CO;2.

Droegemeier, K. K., and R. B. Wilhelmson (1985a), Three-dimensional numerical modeling of convection produced by interacting thunderstorm outflows. Part I: Control simulation and low-level moisture variations, *J. Atmos. Sci.*, *42*(22), 2381–2403, doi:10.1175/1520-0469(1985)042<2381:TDNMOC>2.0.CO;2.

Droegemeier, K. K., and R. B. Wilhelmson (1985b), Three-dimensional numerical modeling of convection produced by interacting thunderstorm outflows. Part II: Variations in vertical wind shear, *J. Atmos. Sci.*, *42*(22), 2404–2414, doi:10.1175/1520-0469(1985)042<2404:TDNMOC>2.0.CO;2.

Jeevanjee, N., and D. M. Romps (2015), Effective buoyancy, inertial pressure, and the mechanical generation of boundary layer mass flux by cold pools, *J. Atmos. Sci.*, *72*(8), 3199–3213, doi:10.1175/JAS-D-14-0349.1.

Khairoutdinov, M. F., and D. A. Randall (2003), Cloud resolving modeling of the arm summer 1997 IOP: Model formulation, results, uncertainties, and sensitivities, *J. Atmos. Sci.*, *60*(4), 607–625, doi:10.1175/1520-0469(2003)060<0607:CRMOTA>2.0.CO;2.

Knupp, K. R., and W. R. Cotton (1982), An intense, quasi-steady thunderstorm over mountainous terrain. Part II: Doppler radar observations of the storm morphological structure, *J. Atmos. Sci.*, *39*(2), 343–358, doi:10.1175/1520-0469(1982)039<0343:AIQSTO>2.0.CO;2.

Langhans, W., and D. M. Romps (2015), The origin of water vapor rings in tropical oceanic cold pools, *Geophys. Res. Lett.*, *42*(18), 7825–7834, doi:10.1002/2015GL065623.

Li, Z., P. Zuidema, and P. Zhu (2014), Simulated convective invigoration processes at trade wind cumulus cold pool boundaries, *J. Atmos. Sci.*, *71*(8), 2823–2841, doi:10.1175/JAS-D-13-0184.1.

Lin, Y.-L., R. D. Farley, and H. D. Orville (1983), Bulk parameterization of the snow field in a cloud model, *J. Clim. Appl. Meteorol.*, *22*(6), 1065–1092, doi:10.1175/1520-0450(1983)022<1065:BPOTSF>2.0.CO;2.

Morrison, H., J. A. Curry, and V. I. Khvorostyanov (2005), A new double-moment microphysics parameterization for application in cloud and climate models. Part I: Description, *J. Atmos. Sci.*, *62*(6), 1665–1677, doi:10.1175/JAS3446.1.

Nie, J., and Z. Kuang (2012), Responses of shallow cumulus convection to large-scale temperature and moisture perturbations: A comparison of large-eddy simulations and a convective parameterization based on stochastically entraining parcels, *J. Atmos. Sci.*, *69*(6), 1936–1956, doi:10.1175/JAS-D-11-0279.1.

Purdom, J. F. W. (1976), Some uses of high-resolution goes imagery in the mesoscale forecasting of convection and its behavior, *Mon. Weather Rev.*, *104*(12), 1474–1483, doi:10.1175/1520-0493(1976)104<1474:SUOHRG>2.0.CO;2.

Rotunno, R., and J. Klemp (1985), On the rotation and propagation of simulated supercell thunderstorms, *J. Atmos. Sci.*, *42*(3), 271–292, doi:10.1175/1520-0469(1985)042<0271:OTRAPO>2.0.CO;2.

Rotunno, R., J. B. Klemp, and M. L. Weisman (1988), A theory for strong, long-lived squall lines, *J. Atmos. Sci.*, *45*(3), 463–485, doi:10.1175/1520-0469(1988)045<0463:ATFSLL>2.0.CO;2.

Schlemmer, L., and C. Hohenegger (2015), Modifications of the atmospheric moisture field as a result of cold-pool dynamics, *Q. J. R. Meteorolog. Soc.*, *142*, 30–42, doi:10.1002/qj.2625.

Seifert, A., and T. Heus (2013), Large-eddy simulation of organized precipitating trade wind cumulus clouds, *Atmos. Chem. Phys.*, *13*(11), 5631–5645, doi:10.5194/acp-13-5631-2013.

Tompkins, A. M. (2001), Organization of tropical convection in low vertical wind shears: The role of water vapor, *J. Atmos. Sci.*, *58*(6), 529–545, doi:10.1175/1520-0469(2001)058<0529:OOTCIL>2.0.CO;2.

Torri, G., and Z. Kuang (2015), A Lagrangian study of precipitation-driven downdrafts, *J. Atmos. Sci.*, *73*, 839–854, doi:10.1175/JAS-D-15-0222.1.

Torri, G., Z. Kuang, and Y. Tian (2015), Mechanisms for convection triggering by cold pools, *Geophys. Res. Lett.*, *42*(6), 1943–1950, doi:10.1002/2015GL063227.

Weaver, J. F., and S. P. Nelson (1982), Multiscale aspects of thunderstorm gust fronts and their effects on subsequent storm development, *Mon. Weather Rev.*, *110*(7), 707–718, doi:10.1175/1520-0493(1982)110<0707:MAOTGF>2.0.CO;2.

Weisman, M. L., and R. Rotunno (2004), "A theory for strong long-lived squall lines" revisited, *J. Atmos. Sci.*, *61*(4), 361–382, doi:10.1175/1520-0469(2004)061<0361:ATFSLS>2.0.CO;2.

Weisman, M. L., J. B. Klemp, and R. Rotunno (1988), Structure and evolution of numerically simulated squall lines, *J. Atmos. Sci.*, *45*(14), 1990–2013, doi:10.1175/1520-0469(1988)045<1990:SAEONS>2.0.CO;2.